nature portfolio

Peer Review File

An Ultraflexible Energy Harvesting-Storage System for Wearable Applications

REVIEWER COMMENTS

Reviewer #1 (Remarks to the Author):

In this work, the authors developed an ultra-flexible Energy Harvesting Storage Systems - FEHSS (integration of flexible organic photovoltaics and zinc ion battery storage) that is applied in wearable electronics. Not only ultra-flexible stand-alone OPV can reach PCE of 16.88% , but also the battery exhibit a high capacity of 6.8 mAh although ultrathin materials of PVA-GO were introduced. The experimental work is carefully performed and conducted giving a comprehensive understanding. There are a few comments for further consideration.

- As the authors introduce ultrathin hydrogel electrolyte of PVA-GO (10um-thick), how does the thickness dependence affecting the overall battery performance? It is also claimed that the PVA-GO hydrogel electrolyte possesses an excellent ionic conductivity, could the authors provide the data of ionic conductivity (mS.cm-1) for the flexible ZIBs.

- “One ZIB can be fully charged within 30 minutes at 100 mW/cm2 and within 1.5 hours at a diminished intensity of 50 mW/cm2” The data of light intensity dependence (different power input) is required for the integrated FEHSS. As wearable devices (most of the time) are subjected to indoor light conditions with the common power input in the range of μW/cm2, low light condition is needed and the capability of the OPV in powering the FEHSS should be presented.

- The manuscript mentions the achievement of a power conversion efficiency (PCE) of up to 16.18% in ultraflexible OPV cells. could the authors provide more details into the optimization of the nanoscale morphology control for enhanced charge transport and collection efficiencies? It is better if the AFM or SEM can be provided. Additionally, incorporating the references to the introduction, (https://doi.org/10.1038/s41467-024-44878-z, https://doi.org/10.1038/s41528-023-00260-5) could contextualize the advancements within the broader research fields of ultraflexible organic solar cells (OSCs).

- Given the dynamic and repetitive mechanical strains expected in wearable applications, it is crucial to understand the durability of the FEHSS components. Could the authors provide a comprehensive analysis of the microstructural changes occurring in both the OPV modules and Zn-ion batteries under such conditions? This analysis could include any observed effects on the electrical performance and mechanical integrity of the system, potentially supported by cyclic bending, stretching tests, and corresponding microscopic examinations before and after the testing.

Reviewer #2 (Remarks to the Author):

The integration of energy harvesters and storage-units is a promising power solution to wearable electronics and the Internet of Things. In this manuscript, the authors report a 90 μm-thick flexible energy harvesting and storage system (FEHSS) consisting of high-performance organic photovoltaics (OPV) modules and Zn-ion batteries. The device exhibited considerable advance in manufacturing process and output performance. And the practical applications have also been well demonstrated. Therefore, it can be considered for publication in Nature Communications after properly addressing the following concerns.

1. There are so many claims: thickness, PCE, stability, power density, organic diodes… Of course, in the integration of OPVs and Zn-ion batteries, various kinds of parameters will be involved. However, a clear statement of the main contribution of this work to the field should be delivered. There are already reports on ultraflexible OPVs (single cell or module), Zn-ion batteries, and the utilization of organic diodes. What is achieved in this work that has never been done before on FEHSS?

2. The OPV module with an effective working area of 6.72 cm2 was fabricated on a 25 cm2 substrate. However, only the area of active layer other than the total device area was used to calculate the areal power output. In this regard, one can easily enlarge the substrate area with a relatively small active layer area to claim higher output power density. Please comment on it.

3. In the integration of FEHSS, is there any optimization process to achieve the best charging parameters, such as the overall efficiency?

4. In Figure 6, the as developed FEHSS was utilized to power an ECG patch and charge a smart phone. What is the light condition of the demonstration? In Figure 6D, some cable connection was hidden by the hand, please replace it with another photograph showing full details. And how about the charging behavior of directly using the OPV module? In current regard, it seems very limited electricity is contributed from the Zn-ion batteries.

5. In Table S2, the highest value of the summarized reported data is 13.61%. However, the state-of-art PCE of reported OPVs has at least reached over 17.07% (1 cm2, 30 January 2023,

https://doi.org/10.1002/eem2.12592). Please show the reported data more objectively. And the information of active materials and substrate area of the modules should be added.

6. Some of the cited references are of lower relevance or unreasonable. Such as in the first sentence of the introduction, "Flexible electronics have produced a paradigm shift in the wearable technology.1" While checking Ref. 1 (Internet of Things is a revolutionary approach for future technology enhancement: a review. Journal of Big data, 2019, 6(1): 1-21.), it is found that the citation of the review is high, however, very little is talking about flexible electronics and wearable technology. And for "This process results in an overall efficiency of 6.61%, which stands among the highest efficiencies reported for variable kinds of FEHSS.8,9" on page 18, as well as in the introduction part, Ref. 8 and Ref. 9 are too old (published in 2013 and 2017, respectively) and all about the integration with Li-ion battery. More recent and relevant papers should be cited to show the advance of this work. It is suggested to list a table to compare the performance of integrated photo-charging devices in the past 5 years.

7. On page 14, line 372, what is polyvinyl alcohol (PVA-GO) hydrogel? Is it fully termed?

We thank the reviewers for recognizing the merits of our manuscript and providing valuable comments for further improvement. We have revised our article following the suggestions. The corresponding changes are itemized below and highlighted (in red) in the revised manuscript.

Response to Reviewers:

Reviewer #1:

In this work, the authors developed an ultra-flexible Energy Harvesting Storage Systems - FEHSS (integration of flexible organic photovoltaics and zinc ion battery storage) that is applied in wearable electronics. Not only ultra-flexible stand-alone OPV can reach PCE of 16.88%, but also the battery exhibit a high capacity of 6.8 mAh although ultrathin materials of PVA-GO were introduced. The experimental work is carefully performed and conducted giving a comprehensive understanding. There are a few comments for further consideration.

Author response:

We appreciate the referee's positive assessment of our work and have addressed the comments point by point as detailed below to further consolidated our research article.

As the authors introduce ultrathin hydrogel electrolyte of PVA-GO (10um-thick), how does the thickness dependence affecting the overall battery performance? It is also claimed that the PVA-GO hydrogel electrolyte possesses an excellent ionic conductivity, could the authors provide the data of ionic conductivity (mS.cm-1) for the flexible ZIBs.

Author response:

We appreciate the reviewer for the insightful questions. The thickness of gel-based electrolytes in batteries plays a crucial role, affecting not only the electrolyte's conductivity but also the time required for ion diffusion. In response to these questions, we have conducted additional electrochemical performance evaluations with hydrogels of different thicknesses. These additional findings have been implemented in the Supplementary Information as Nyquist plots (**Figure S5A**). Besides, we have extracted the ionic conductivity of the PVA-GO hydrogel with thicknesses of 10 µm, 100 µm, and 1 mm, following the equation:

$$\sigma = \frac{L}{R \times S}$$

where L stands for the hydrogel thickness (i.e., the distance between the two electrodes), R stands for the bulk resistance of the hydrogel, and S stands for the area of electrode/electrolyte interface. The extracted values are 7.0, 6.7, and 6.2 mS cm^{-1} for the hydrogel with thicknesses of 10 µm, 100 µm, and 1 mm, respectively. We've enriched the main text with discussion on how hydrogel thickness influences ZIB performance, as detailed below:

[page 15, line 28]

To quantitatively investigate the impact of hydrogel thickness in the performance of ZIBs, we conducted electrochemical evaluations of hydrogels with different thicknesses, i.e., 10 µm, 100 µm, and 1 mm. Nyquist plots (**Figure S5A**) depict the corresponding battery performance under open circuit voltage conditions. The intercepts of these curves reveal an increase in ohmic resistance from 2.7 Ω to 81 Ω as the hydrogel thickness increases from 10 µm to 1 mm. The ionic conductivity (σ) of hydrogel electrolytes was then calculated following:

$$\sigma = \frac{L}{R \times S} \tag{3}$$

where L stands for the hydrogel thickness (i.e., the distance between the two electrodes), R stands for the bulk resistance of the hydrogel, and S stands for the area of electrode/electrolyte interface. The ionic conductivities were determined to be 7.1, 6.7, and 6.2 mS cm^{-2} for the hydrogel with thicknesses of 10 µm, 100 µm, and 1 mm, respectively. Reducing the thickness of hydrogels generally enables faster ion diffusion between the anode and cathode by shortening the distance and reduces the impedance resistance.

While the reduction in electrolyte thickness enhances ionic conductivity, it may concurrently have a negative impact on battery capacity (Q). The voltage-capacity curves illustrated in **Figure 4E** reveal a 4.5% decrease in discharge capacity when the hydrogel thickness decreases from 1 mm to 10 µm. This reduction in capacity may be attributed to the limited electrolyte volume and ion availability in thinner hydrogels compared to their thicker counterparts. Moreover, ultrathin hydrogel electrolytes are likely to more rapidly saturate with active ions at the electrode-electrolyte interface, constraining the ions available for electrochemical reactions, which could, in turn, decrease specific battery capacity and discharge duration. Despite the relatively lower capacity of the ultrathin battery, it remains adequate for most wearable applications. The significant benefits in flexibility offered by ultrathin electrolytes compensates for the minor capacity losses. Consequently, the 10 µm hydrogel electrolyte was chosen for our FEHSS, prioritizing its exceptional flexibility and ionic conductivity.

(Note: references are omitted herein for clarity. Please refer to the revised manuscript for details.)

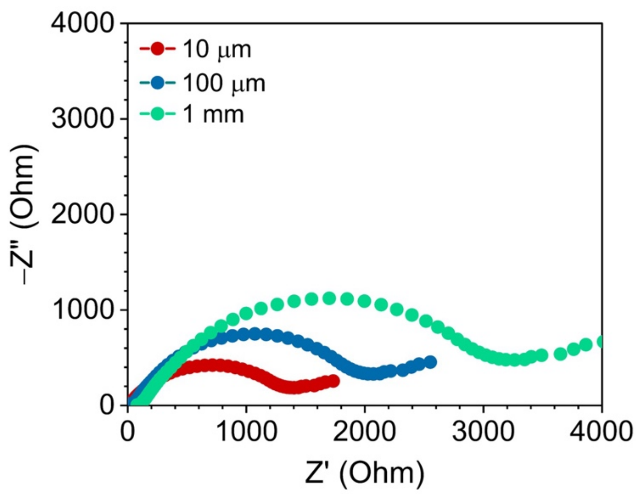

Figure S5A. (A) Nyquist plots of ZIBs featuring hydrogel electrolyte of different thicknesses: 10 μm (red), 100 μm (blue), and 1 mm (cyan).

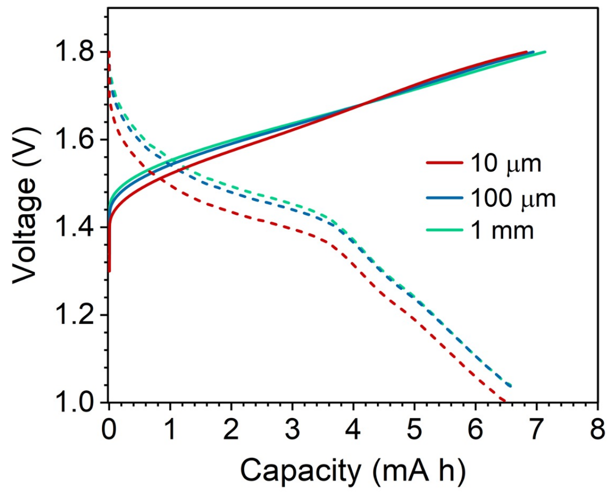

Figure 4E. Voltage-capacity profile of flexible Zn-MnO_2 batteries, featuring hydrogel electrolyte thicknesses of 10 μm (red), 100 μm (blue), and 1 mm (cyan), charged by an external power supply.

Table R1. The dependence of ionic conductivity and battery capacity on the thickness of hydrogel electrolytes.

Hydrogel thickness	Ionic conductivity (mS cm^{-2})	Capacity (mA h)
10 μm	7.1	6.82
100 μm	6.7	6.95
1 mm	6.2	7.14

One ZIB can be fully charged within 30 minutes at 100 mW/cm2 and within 1.5 hours at a diminished intensity of 50 mW/cm2". The data of light intensity dependence (different power input) is required for the integrated FEHSS. As wearable devices (most of the time) are subjected to indoor light conditions with the common power input in the range of µW/cm2, low light condition is needed and the capability of the OPV in powering the FEHSS should be presented.

Author response:

We appreciate this valuable suggestion. Indeed, evaluation of the FEHSS performance under indoor light conditions are critical for practical applications. We have conducted further research on the charging rate dependence with varying the lighting conditions and implemented the results in revised **Figure S8**. The relevant discussions and figures are show as follows:

[page 19, line 31]

We further evaluate the charge-discharge profiles of the FEHSS under varying light intensities to simulate outdoor and indoor lighting conditions and assess performance impacts. The charging rate generally declines with a decrease in the output current of the OPV module, which correlates directly with reduced light intensities (**Figure S8)**. As depicted in **Figure S8A**, under 1 sun illumination, i.e., light intensity of 100 mW cm^{-2}, a ZIB integrated with a 6.72 cm^2 OPV module can be fully charged within 37 minutes (black), and within 72 min at a reduced intensity of 50 mW cm^{-2} (blue). Indoor light levels typically range from 500-700 lux, translating to approximately 75-100 µW cm^{-2}.[77] A notable increase in charging time is observed as the light intensity is decreased to indoor light conditions (**Figure S8B**). As light intensity diminished from 1000 µW cm^{-2} to 75 µW cm^{-2}, the charging duration of the same ZIB escalated from approximately 400 minutes to 580 minutes. Although full charging to 1.8 V indoors exceeds 6.5 h, the system exhibits a noteworthy interim charging capability. Within 2 h, the ZIB battery can be partially charged to 1.5 V, becoming capable of powering low-energy devices. The integration with an OPV module facilitates continuous charging, even under low lighting conditions, enhancing the system's versatility and utility for both outdoor and indoor applications.

(Note: reference is omitted herein for clarity. Please refer to the revised manuscript for details.)

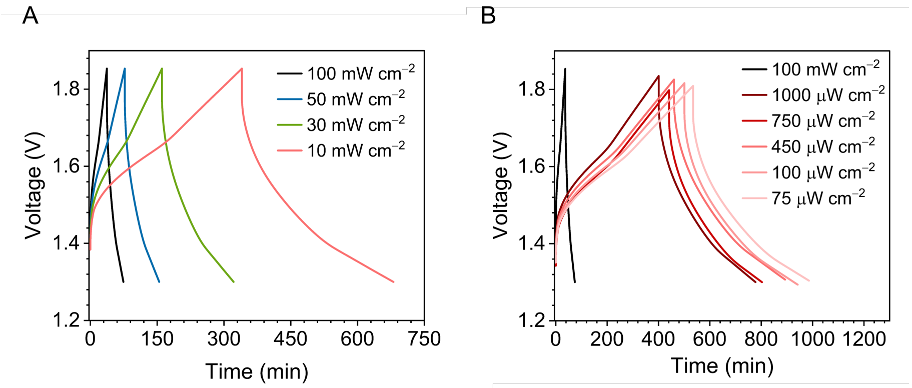

Figure S8. (A) Charge-discharge profiles of the FEHSS under different light intensities. (B) Charge-discharge profiles of FEHSS under low light intensities approximating indoor light conditions (red traces), in comparison with the profile obtained under 1 sun illumination condition, i.e., 100 mW cm^{-2} (black). The FEHSS consists of a 6.72 cm^2 ultraflexible OPV module, and a ZIB battery.

The manuscript mentions the achievement of a power conversion efficiency (PCE) of up to 16.18% in ultraflexible OPV cells. could the authors provide more details into the optimization of the nanoscale morphology control for enhanced charge transport and collection efficiencies? It is better if the AFM or SEM can be provided. Additionally, incorporating the references to the introduction, (https://doi.org/10.1038/s41467-024-44878-z, https://doi.org/10.1038/s41528-023-00260-5) could contextualize the advancements within the broader research fields of ultraflexible organic solar cells (OSCs).

Author response:

We thank the reviewer for this insightful suggestion.

1) To better understand the nanoscale morphology of the binary and ternary blends and their impact on the charge transport efficiency, we performed grazing incidence wide-angle X-ray scattering (GIWAXS) measurements. The experimental results as shown in revised **Figure 2**, and the relevant discussions are detailed below:

[page 8, line 23]

To better understand the microstructure of the binary and ternary blends, we perform grazing incidence wide-angle X-ray scattering (GIWAXS). **Figure 2F-G** show the 2D GIWAXS data of binary blend (**Figure 2F**) and ternary blend (**Figure 2G**) films, with their cake cut profiles presented in **Figure 2H**. Note that the peak at 0.47 Å^{-1} is from the Kapton foil, which is used to seal the measurement chamber. Both samples show a (100) scattering peak at 0.30 Å^{-1}, which is ascribed to the lamellar stacking of PM6. π-π stacking peaks are observed at 1.70 Å^{-1} in the binary blend and at 1.73 Å^{-1} in the ternary blend. A slight enhancement and peak shift in the π-π stacking peak is observed in PM6:O-IDTBR:Y6 ternary system from 1.70 Å^{-1} to 1.73 Å^{-1} in the out-of-plane (OOP) direction, corresponding to a shrinkage of π-π distance from 3.70 Å to 3.63 Å. Both the increased intensity and peak shift to a higher q value are beneficial for the OPV use as a closer π-π stacking distance and more crystallites can cause faster and more efficient charge carrier transfer and transport.

(Note: reference is omitted herein for clarity. Please refer to the revised manuscript for details.)

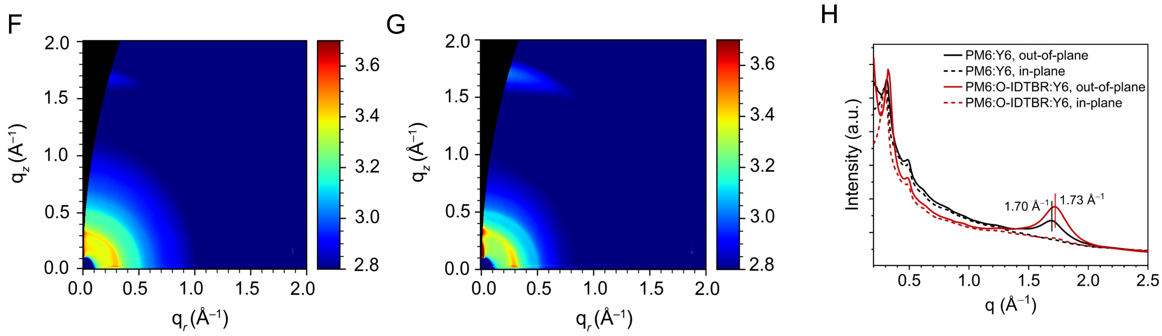

Figure 2. (**F**) 2D GIWAXS data of PM6:Y6 binary blend. (**G**) 2D GIWAXS data of PM6:O-IDTBR:Y6 ternary blend. (**H**) Cake cuts from 2D GIWAXS data of the binary blend (black) and the ternary blend (red). Cake cuts in IP and OOP directions are shown in dashed and solid lines, respectively.

2) Besides, we have investigated the nanoscale morphology of the binary and ternary blends using atomic force microscopy (AFM), with their results summarized below. The AFM images do not reveal obvious differences in the surface topography of the binary and ternary blend active layers.

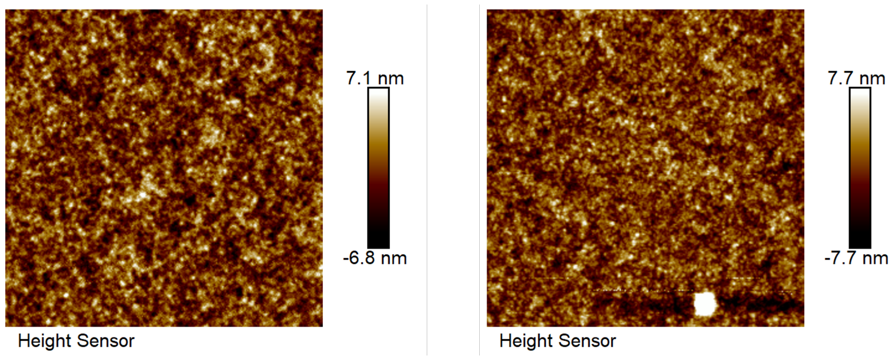

Figure R1. AFM topography images of the PM6:Y6 binary blend (left) and the PM6:O-IDTBR:Y6 ternary blend (right).

3) We acknowledge the reviewer for the suggested literature. We have added suggested articles in the introduction section, as detailed below:

[page 3, line 29]

Recent investigations have substantially escalated the power conversion efficiency (PCE) of flexible OPVs, propelling it beyond the 10% threshold.[20-23] Simultaneously, intense efforts have been made to enhance the performance robustness to withstand harsh outdoor conditions.[22,24-26]

Given the dynamic and repetitive mechanical strains expected in wearable applications, itis crucial to understand the durability of the FEHSS components. Could the authors provide a comprehensive analysis of the microstructural changes occurring in both the OPV modules and Zn-ion batteries under such conditions? This analysis could include any observed effects on the electrical performance and mechanical integrity of the system, potentially supported by cyclic bending, stretching tests, and corresponding microscopic examinations before and after the testing.

Author response:

We appreciate the reviewer's valuable suggestion. Indeed, evaluation of the device performance when subjected to repetitive mechanical strains is of paramount importance for practical applications. Following the suggestion, we have added further experiments and discussions for OPV modules, Zn-ion batteries, and integrated FEHSS, as detailed below:

1) For OPV modules, we reported their electrical performance after cyclic bending and stretching tests, as depicted in **Figure 3F**. In the revised manuscript, we have further implemented SEM characterizations to visualize the mechanical durability at a microscopic level. The results have been added to revised **Figure S4**.

[page 13, line 1]

"The ultraflexible OPV modules displayed exceptional mechanical durability. As shown in **Figure 3F**, after being bent to a 1 mm radius for 1000 cycles, the 6.72 cm^2 module retained 90% of its original power output. In additional test, the module was attached to a pre-stretched rubber membrane and then allowed to release which introduced a compressive strain of 50%. After 1000 cycles of compression-stretching, the module continued to generate 50 mW of power, maintaining its current and voltage output at 9.8 mA and 6.4 V, respectively."

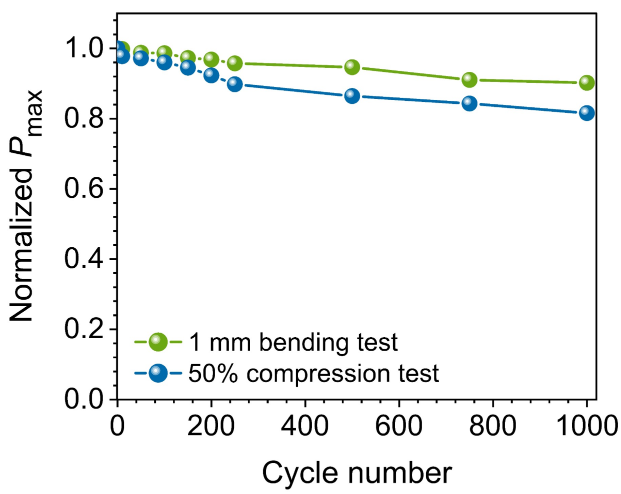

Figure 3. (F) Mechanical durability of the 6.72 cm^2 module tested under a bending radius of 1 mm (green) and under 50% compression strain (blue) for 1000 stretching cycles.

[page 13, line 11]

Scanning electron microscopic (SEM) images of the OPV module before and after subjected to the mechanical durability test are depicted in **Figure S4B-C**. Following the continuous bending test for 1000 cycles, there was a noticeable increment in the formation of wrinkles across the surface of the ultraflexible OPV module. On the other hand, there were no visible manifestations of cracking or interfacial delamination within the examined regions. These observations together with the performance stability are indicative of the OPV module's resilience to mechanical strains.

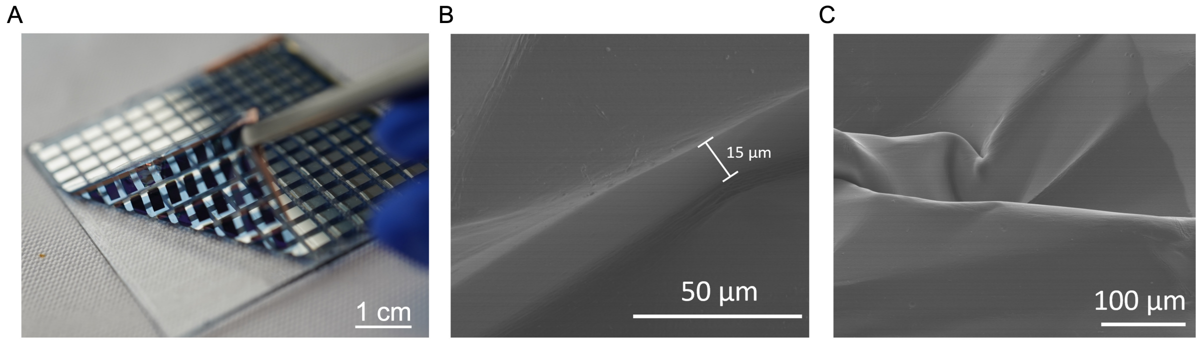

Figure S4. (A) Photograph of a 5x5 cm^2 OPV module being delaminated from the supporting glass slide. (B-C) Scanning electron microscopic (SEM) images of an ultraflexible OPV before (B) and after (C) the mechanical durability test of 1000 bending cycles at 1 mm bending radius.

2) For the ZIBs, we have conducted additional experiments to assess its mechanical durability. The outcomes of these new experiments have been incorporated into the revised **Figure S5** and **Figure S6**. The supplementary discussion in the main text is presented below:

[page 17, line 20]

The mechanical robustness of ultrathin ZIBs is pivotal for their practical application across various wearable scenarios. The 85 µm-thick ZIB exhibits excellent mechanical stability, retaining 88% of its original coulombic efficiency after being subjected to 500 continuous bending cycles at a bending radius of 1 mm (**Figure S5E**). To further assess the effects of bending strain on the battery's performance, we analyzed Nyquist plots obtained before and after the bending experiments. As shown in **Figure S5F**, a modest increase in the ohmic resistance (approximately 5%) and the charge transfer resistance (around 8.5%) was observed, suggesting subtle performance alterations. SEM images presented in **Figure S6** provide visual elucidation of the battery's structural integrity before and after the bending test. These findings collectively suggest the robust mechanical resilience of the ultrathin ZIB, capable of enduring multiple bending cycles without significant performance degradation.

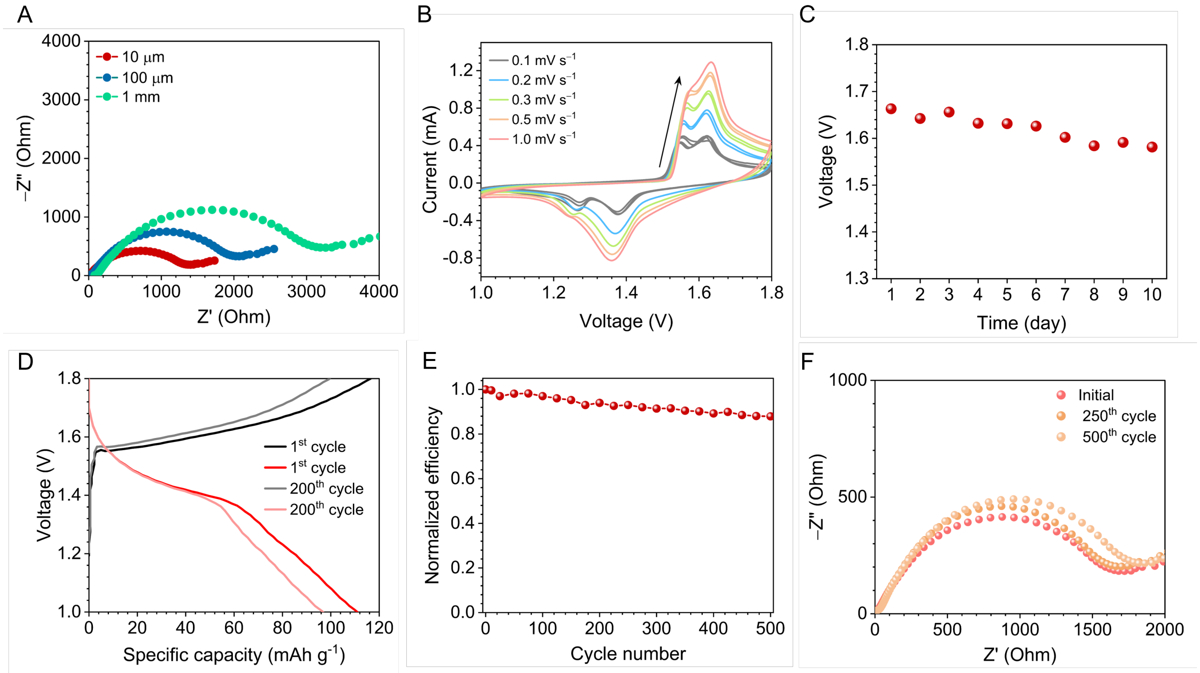

Figure S5. (A) Nyquist plots of ZIBs featuring hydrogel electrolyte of different thicknesses: 10 µm (red), 100 µm (blue), and 1 mm (cyan). (B) Cyclic voltammogram of an 85 µm-thick ZIB at variable scan rates. (C) Storage stability of the 85 µm-thick flexible ZIB under ambient conditions. (D) Charge-discharge curves of a flexible ZIB at both the 1st and 200th cycles. (E) Coulombic efficiency of the 85 µm-thick ZIB recorded over continuous bending cycles at a bending radius of 1 mm. The results highlight mechanical durability of the thin ZIB. (F) Nyquist plots of the 85 µm-thick ZIB after subjected to 250 and 500 bending cycles (orange), contrasting with its initial unstrained state (red).

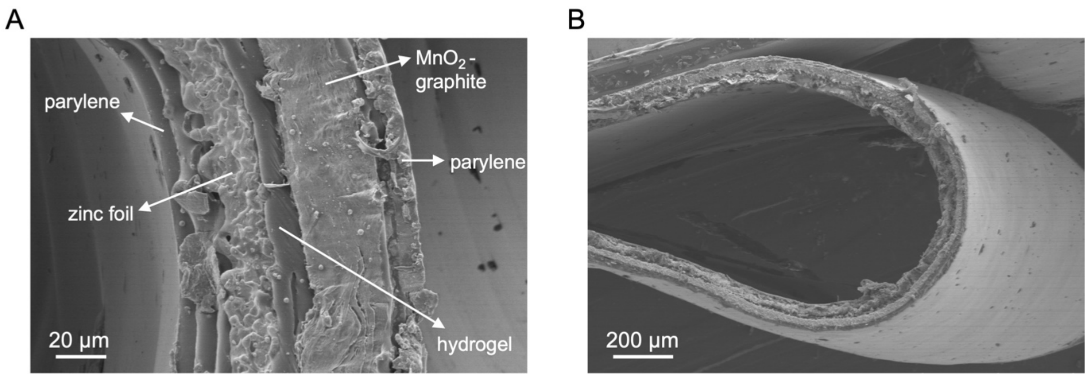

Figure S6. SEM images of a sub-100 µm thick ZIB. (A) Cross-sectional SEM image of the as-prepared ZIB, highlighting each layer component. (B) Cross-sectional SEM image of the ZIB under bending strain, demonstrating mechanical compliance and structural integrity.

3) For the integrated FEHSS, we reported their electrical performance after cyclic bending and stretching tests, as depicted in **Figure 1G**. In the revised manuscript, we have further implemented SEM characterizations to visualize its mechanical durability. The results have been added to revised **Figure S9**.

[page 5, line 29]

"Bent to a radius of less than 1 mm for 500 cycles or being compressed to a strain of 10% for 100 cycles, the FEHSS maintains over 80% of its overall power conversion and storage efficiency (**Figure 1G**), showing mechanical durability for practical applications."

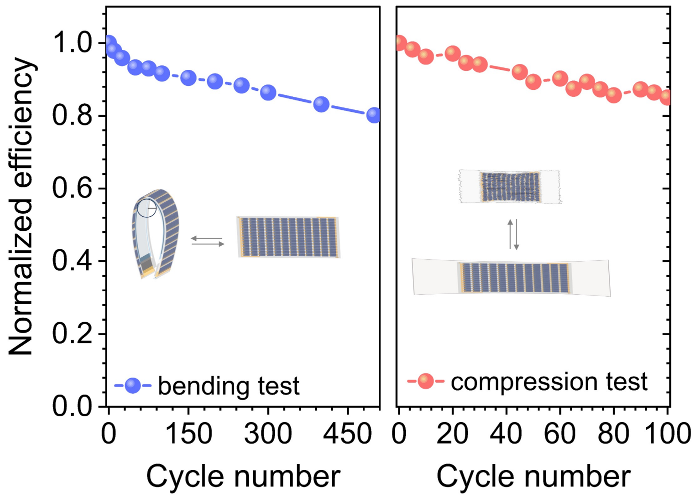

Figure 1. (G) Mechanical durability of the FEHSS for over 500 cycles under a 1 mm bending radius (left), and 100 cycles of compression-stretching under 10% strain (right). The y-axis shows the normalized efficiency of photo-conversion and storage.

[page 21, line 8]

…Under mechanical strain, such as bending to a 1 mm radius over 500 cycles or enduring repeated 10% compression strain for 100 cycles, the system preserves over 80% of its original light harvesting-storage efficiency (**Figure 1G**). It sustains a voltage output of 1.48 V and a capacity exceeding 5.3 mA h. **Figure S9** depicts cross-sectional SEM images of the as-prepared FEHSS (**Figure S9A**), FEHSS under bending strain (**Figure S9B**), and after cyclic bending test (**Figure S9C**). The ultrathin FEHSS can achieve a bending radius as low as 120 μm (**Figure S9B**). Following 500 cycles of repeated bending test, slight deformation and kinks were observed at the battery side within the FEHSS, which might be the major cause of the performance loss. Enhancement of the interfacial strength among layers in the battery could mitigate the observed deformation, representing a potential avenue for future optimization.

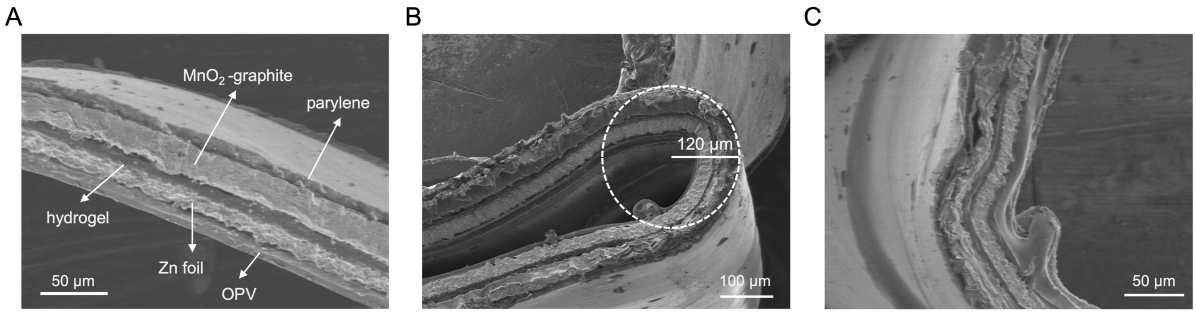

Figure S9. SEM images of integrated FEHSS. (A) Cross-section SEM image of an as-prepared FEHSS, highlighting each layer component. (B) Cross-sectional SEM image of the FEHSS under bending strain, demonstrating a bending radius down to 120 µm. (C) Cross-sectional SEM image of the FEHSS after 500 cycles of repeated bending test.

Reviewer #2 (Remarks to the Author):

The integration of energy harvesters and storage-units is a promising power solution to wearable electronics and the Internet of Things. In this manuscript, the authors report a 90 μm-thick flexible energy harvesting and storage system (FEHSS) consisting of high-performance organic photovoltaics (OPV) modules and Zn-ion batteries. The device exhibited considerable advance in manufacturing process and output performance. And the practical applications have also been well demonstrated. Therefore, it can be considered for publication in Nature Communications after properly addressing the following concerns.

Author response:

We appreciate the referee's positive assessment of our work and have addressed the comments point by point as detailed below.

1. There are so many claims: thickness, PCE, stability, power density, organic diodes... Of course, in the integration of OPVs and Zn-ion batteries, various kinds of parameters will be involved. However, a clear statement of the main contribution of this work to the field should be delivered. There are already reports on ultraflexible OPVs (single cell or module), Zn-ion batteries, and the utilization of organic diodes. What is achieved in this work that has never been done before on FEHSS?

Author response:

We appreciate the reviewer for this insightful comment, and for promoting a clearer articulation of the main contributions of our work. We recognize the prolific advancements within the domains of OPVs, Zn-ion batteries, and the strategic use of organic diodes individually. However, our work distinguishes itself by combining these technologies into a cohesive system that addresses specific limitations in the current understanding and application of FEHSS. In the revised manuscript, we have strengthened our major claim in the following aspects:

1) The necessity of FEHSS over individual OPVs or ZIBs:

[page 24, line 21]

While individual energy harvesting and storage components can function independently, their integration addresses inherent limitations. In FEHSS, the OPV module continuously charges the battery, thereby prolonging its lifespan, while the battery ensures power provision under low-light conditions when the OPV's output is insufficient. Visual evidence of this synergy is provided in **Videos S2** and **S3**. When the LED is powered solely by the OPV, its operation relies on high light intensity and ceases once the incident light diminishes (**Video S2**). Utilizing FEHSS effectively circumvents this limitation, as the ZIB within the FEHSS sustains the LED's brightness even in darkness (**Video S3**). These scenarios highlight the critical importance of integrating both the OPV and ZIB within a unified system.

2) The advantage of our FEHSS over other documented systems:

To reinforce the significance of our main achievement, we have conducted a comparative analysis on the performance metrics between our FEHSS and previously reported systems. This comparison is succinctly presented in a Radar chart (**Figure 5I)** and a summary table (**Table S4**). The addition of this discussion, along with the updated figure and table, are elaborated below:

[page 21, line 18]

The radar chart depicted in **Figure 5I**, along with the summarized performance metrics in **Table S4**, provides a comprehensive overview of the documented FEHSS based on photovoltaic energy harvesters and battery storage systems. Noteworthy among these systems is our FEHSS, distinguished by its unparalleled flexibility, exceptional electrical performance, and inherent safety features. Demonstrating mechanical compliance with a bending radius down to 120 μm, our system maintains robust functionality across both individual battery and OPV modules, as evidenced by excellent PCE, energy density, specific capacity, and overall energy harvesting-storage efficiency. The common trade-offs between electrical and mechanical performance within these systems have been effectively addressed. Moreover, our FEHSS stands out from other documented systems with the incorporation of a current management diode, a feature enhancing its practical applicability. These findings highlight the efficiency and versatility of our FEHSS, positioning it as a promising solution for wearables applications.

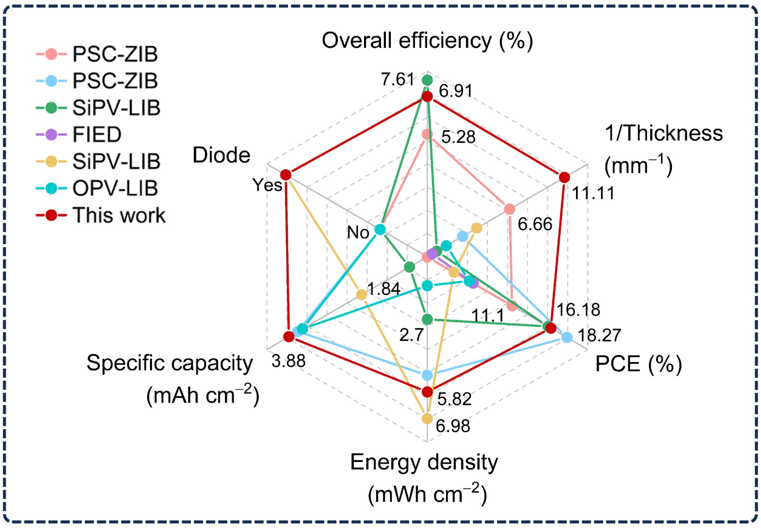

Figure 5I. Radar plot comparing the performance metrics of reported FEHSSs based on solar energy harvesting and battery storage. PCS-ZIB stands for a perovskite solar cell integrated with a zinc-ion battery, SiPV-LIB stands for a silicon photovoltaic integrated with a lithium-ion battery, FIED stands for a fiber-shaped integrated energy device, and OPV-LIB represents an organic photovoltaic integrated with a lithium-ion battery.

Table S4. Summary of the performance of reported FEHSSs based on solar energy harvesters and battery storage systems.

FEHSS type	1/Thickness (mm^{-1})	PCE (%)	Energy density (mWh cm^{-2})	Specific capacity (mAh cm^{-2})	Diode	Overall efficiency (%)	Ref.
PSC-ZIB	6.66	11.1	0.0016	-	No	5.28	26
PSC-ZIB	2.85	18.27	5.11	3.63	No	-	27
SiPV-LIB	0.77	15.8	2.7	0.5	No	7.61	28
SiPV-LIB	0.4	6	6.98	1.84	No	-	29
FIED	3.85	3.5	-	-	Yes	-	30
OPV-LIB	4.0	5.49	1.25	3.5	No	-	31
OPV-ZIB	11.1	16.18	5.82	3.88	Yes	6.91	This work

Note: PSC stands for perovskite solar cell, ZIB stands for zinc-ion battery, SiPV stands for silicon photovoltaic, LIB stands for lithium-ion battery, FIED stands for fiber-shaped integrated energy device, OPV stands for organic photovoltaic.

In summary, although individual components may have been documented previously, the comprehensive integration within an ultrathin configuration and demonstrated real-world applicability of our FEHSS represent a significant innovation. We believe our work not only advances the state of the art but also paves the way for new practical implementations of flexible and efficient hybrid energy systems.

2. The OPV module with an effective working area of 6.72 cm2 was fabricated on a 25 cm2 substrate. However, only the area of active layer other than the total device area was used to calculate the areal power output. In this regard, one can easily enlarge the substrate area with a relatively small active layer area to claim higher output power density. Please comment on it.

Author response:

We appreciate the reviewer for this insightful comment.

1) The fabrication of the 25 cm^2 OPV module entails the integration of 168 individual cells, each with a nominal active area of 0.04 cm^2. To ensure optimal performance and mitigate crosstalk among adjacent cells arising from shadow effects during thermal deposition of the ITO and subsequent top electrode layers, a suitable gap of approximately 0.5-1 mm is necessary and maintained between cells. Additionally, the implementation of serial and parallel connections necessitates the incorporation of external wiring between cells, further contributing to the module's overall dead area. For direct comparison with reported systems,

the P_{areal} of all references mentioned in **Table S2** were calculated with the effective device area instead of the substrate area.

2) The decision to utilize a larger substrate area (i.e., 5× 5 cm^2) in our study was motivated by the need to accommodate multiple batteries for voltage enhancement, as we adopted a vertical integration between OPV and ZIBs, and an in-plane integration among ZIBs. Aligning the total substrate area facilitates the integration, thus enhancing overall system performance.
3) It is acknowledged that the presence of dead areas could potentially influence the calculations of module power density and overall efficiency. To address this concern and optimize substrate area utilization, alternative fabrication techniques like laser patterning and photolithography, compatible with ultrathin plastic substrates, could be explored. These methods hold promise for reducing dead areas and wiring space, thereby maximizing effective working area, and enhancing power density normalized by total substrate area. While we appreciate the importance of such efforts, they fall outside the main scope of current work. We intend to dedicate efforts to explore these avenues in future research endeavours.

3. In the integration of FEHSS, is there any optimization process to achieve the best charging parameters, such as the overall efficiency?

Author response:

We thank the reviewer for this valuable question. Following the definition of the overall photo-electric conversion and storage efficiency ($E_{overall}$),

$$E_{overall} = \frac{Q \times V}{I \times A_{OPV} \times t_{charge}} \times 100 \quad (5)$$

where I is the light intensity, A_{OPV} is the effective OPV area, and t_{charge} is the photo-charging time (in hours), we have investigated how the parameters like I, A_{OPV}, and t_{charge} influence the overall efficiency. We found that $E_{overall}$ of FEHSS is intricately linked to incident light intensity I, which directly influences the current output of the OPV module and subsequently impacts the charging time of the battery. This charging rate, in turn, influences the battery's capacity and, consequently, its discharge energy density. Achieving optimal efficiency requires balancing light intensity conditions to minimize charging time while maximizing capacity and discharge energy density. The discussions for the mentioned factors are now implemented in the revised manuscript and a new table in Supplementary information (**Table S3**), detailed below:

[page 20, line 17]

In an outdoor environment with a light intensity of approximately 65 mW cm^{-2}, an FEHSS comprised of a 1.28 cm^2 OPV module and a ZIB can be spontaneously charged to a capacity of 5.5 mA h within 1.5 hours. This process results in an overall efficiency of 6.61%. With a reduced light intensity of 10 mW cm^{-2}, the same FEHSS can be charged to a capacity of 5.9 mA h within 10 hours, yielding an overall efficiency of 6.91%, which stands among the highest efficiencies reported for variable kinds of FEHSS. Supplementary **Table S3** provides a comprehensive evaluation of the photo-charging capabilities of FEHSS under various light intensities, specifically detailing performance metrics with small (1.28 cm^2) and relatively large (6.72 cm^2) OPV modules. Increased incident light intensities generally correlate with faster charging rates for both sizes of OPV modules. Nonetheless, this acceleration in charging rates inversely affects the battery's capacity. As the light intensity diminished from 100 mW cm^{-2} to 10 mW cm^{-2}, the overall efficiency with a 1.28 cm^2 OPV module raised from 5.27% to 6.91%. Above results suggest that both the charging rate and the overall efficiency of FEHSS are intricately linked to the incident light intensity *I*, which directly influences the current output of the OPV module and subsequently impacts the charging behaviour of the battery. A balance must therefore be achieved between charging rate and overall efficiency, as excessively low charging rate may limit the practical utility of the integrated energy system.

Table S3. Overall efficiency of FEHSS with one ZIB when charged under different light intensities.

OPV module	Light intensity (mW cm^{-2})	Charging time (hours)	Capacity (mAh)	Energy density (mWh cm^{-2})	Overall efficiency (%)
6.72 cm^2	100	0.6	3.0	2.65	1.15
	65	0.95	3.5	3.00	1.25
	50	1.2	3.7	3.14	1.35
	30	2.0	3.8	3.25	1.41
	10	5.6	4.0	3.42	1.59
1.28 cm^2	100	1.0	5.27	4.5	5.27
	65	1.5	5.5	4.7	6.61
	50	2.0	5.7	4.89	6.68
	30	3.3	5.8	4.97	6.86
	10	10	5.9	5.05	6.91

4. In Figure 6, the as developed FEHSS was utilized to power an ECG patch and charge a smart phone. What is the light condition of the demonstration? In Figure 6D, some cable connection was hidden by the hand, please replace it with another photograph showing full details. And how about the charging behavior of directly using the OPV module? In current regard, it seems very limited electricity is contributed from the Zn-ion batteries.

Author response:

We appreciate the valuable questions.

1) The light condition of the demonstrations in **Figure 6A-D** was natural sunlight outside in the afternoon, with an estimated intensity of 65 mW cm^{-2}. The light condition for demonstrations in **Figure 6E** was 1 sun under a solar simulator.
2) We have included an extra photograph as Supplementary **Figure S10C**, depicting the cable connection layout in detail. We believe this addition will provide readers with enhanced clarity on the demonstration in **Figure 6D**. In "Methods" section, we have explained the methodology, stating that "the smartphone charging was conducted by connecting the FEHSS to a smartphone using a type-C cable, and an additional direct current to direct current (DC-DC) converter to regulate the voltage stably at 5.0 V.

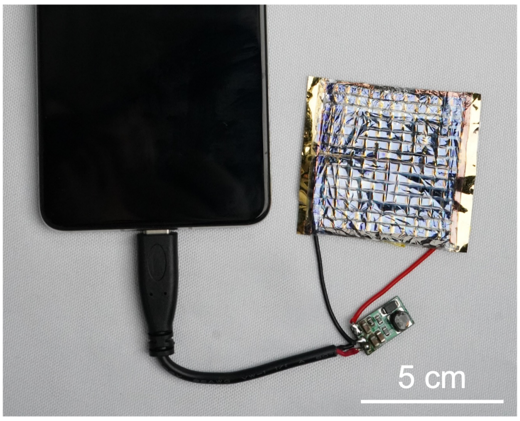

Figure S10C. Photograph showing the system layout for charging a smartphone by FEHSS. The printed regulation board consists of a DC-DC converter to stabilize the voltage output at 5.0 V.

3) In response to the last question, we have added an additional demonstration, as Supplementary **Video S2** and **Video S3**, that highlight the importance of both components in the integrated system. We have incorporated discussions regarding this in the main text, as detailed below:

[page 24, line 21]

While individual energy harvesting and storage components can function independently, their integration addresses inherent limitations. In FEHSS, the OPV module continuously charges the battery, thereby prolonging its lifespan, while the battery ensures power provision under low-light conditions when the OPV's output is insufficient. Visual evidence of this synergy is provided in **Videos S2** and **S3**. When the LED is powered solely by the OPV, its operation relies on high light intensity and ceases once the incident light diminishes (**Video S2**). Utilizing FEHSS effectively circumvents this limitation, as the ZIB within the FEHSS sustains the display's brightness even in darkness (**Video S3**). These scenarios underscore the critical importance of integrating both the OPV and ZIB within a unified system.

5. In Table S2, the highest value of the summarized reported data is 13.61%. However, the state-of-art PCE of reported OPVs has at least reached over 17.07% (1 cm^2, 30 January2023, https://doi.org/10.1002/eem2.12592). Please show the reported data more objectively. And the information of active materials and substrate area of the modules should be added.

<u>Author response</u>:

We appreciate the reviewer for this valuable comment. Indeed, we have overlooked the latest innovations of flexible OPVs based on PET and PEN substrates. In response, we have revised **Table S2**, incorporating more recent representative work. We have introduced one more column labeled "PCE" alongside "P_{areal}" to facilitate a comprehensive comparison. Notably, we observed that the reported high performance exceeding 15% were mainly based on 125 µm substrate, falling beyond the defined "ultraflexible" OPVs category with thickness below 10 µm. Nevertheless, we genuinely appreciate the reviewer's suggestion to include reported data objectively.

Table S2. Summary on the performance of reported flexible OPVs and flexible OPV modules.

	Thickness (µm)	Active area (cm^2)	P_{areal} ($mW\ cm^{-2}$)	Active materials	Substrate	Ref
Flexible OPVs	175	1	7.17	PTB7-Th:p-DTS(FBTTH2)2:$PC_{71}BM$	PET	1
	175	2	5.66	PTB7:PC_{71} BM	PET	2
	175	10	5.83	PTB7-Th:p-DTS(FBTTH2)2:$PC_{71}BM$	PET	3
	125	1	17.07	PM6:L8-BO	PET	4
	125	1	16.71	PBDB-TF: BTP-eC9	PEN	5
	125	1	16.54	PM6:BTP-4Cl-12	PET	6
	125	1	15.82	PM6:BTP-eC9:$PC_{71}BM$	PET	7
	125	1	14.29	PM6:Y6	PET	8
	125	1	13.61	PM6:Y6	PET	9

	125	1	12.26	PBDB-TF:IT-4F	PET	10
	125	1	12.16	PTB7-Th: COi8DFIC:$PC_{71}BM$	PET	11
	125	1	3.52	PBDTTTz-4:$PC_{71}BM$	PET	12
	125	1	2.25	PTB7-TH : $PC_{61}BM$	PET	13
	125	1	2.7	P3HT:$PC_{71}BM$	PET	14
	125	1	1.93	BDTTT-C-T: $PC_{71}BM$	PET	15
	125	1.04	9.77	PBDB-T:ITIC	PET	16
	125	1.2	5.85	P3HT:ICBA	PET	17
	125	4	7.09	PTB7:$PC_{71}BM$	PET	18
	125	4	1.93	P3HT:$PC_{71}BM$	PEN	19
Ultra-flexible OPVs	2.5	1.94	6.97	PTzNTz:$PC_{71}BM$	PI/Ag	20
	3	1	8.8	PBDTTT-OFT:$PC_{71}BM$	Parylene	21
	3	1.2	5.85	PTzNTZ-BOBO:$PC_{71}BM$	Parylene	22
	3	1.36	11.46	PBDBT:ITIC	PI	23
	3	2.97	8.43	PBDTTT-OFT: IEICO-4F	Parylene	24
	4	3.2	8.08	PM6:IT-4F	Parylene	25
	4	1.28	13.8	PM6:O-IDTBR:Y6	Parylene	This work
		6.72	10.3	PM6:O-IDTBR:Y6	Parylene	
		16	4.9	PM6:O-IDTBR:Y6	Parylene	

6. Some of the cited references are of lower relevance or unreasonable. Such as in the first *sentence of the introduction, "Flexible electronics have produced a paradigm shift in the wearable technology.1" While checking Ref. 1 (Internet of Things is a revolutionary approach for future technology enhancement: a review. Journal of Big data, 2019, 6(1): 1-21.), it is found that the citation of the review is high, however, very little is talking about flexible electronics and wearable technology. And for "This process results in an overall efficiency of 6.61%, which stands among the highest efficiencies reported for variable kinds of FEHSS.8,9" on page 18, as well as in the introduction part, Ref. 8 and Ref. 9 are too old (published in 2013 and 2017, respectively) and all about the integration with Li-ion battery. More recent and relevant papers should be cited to show the advance of this work. It is suggested to list a table to compare the performance of integrated photo-charging devices in the past 5 years.*

Author response:

We appreciate the reviewer for careful reading and the insightful suggestions.

1) Indeed, the references in the beginning sentences of Introduction are not highly representative. We have revised the cited references that are more relevant, as listed below:

[1] Gao, W., Ota, H., Kiriya, D., Takei, K. & Javey, A. Flexible electronics toward wearable sensing. *Acc. Chem. Res* **52**, 523-533, (2019).

[2] Someya, T., Bao, Z. & Malliaras, G. G. The rise of plastic bioelectronics. *Nature* **540**, 379-385 (2016).

[3] Rogers, J., Bao, Z. & Lee, T. W. Wearable bioelectronics: opportunities for chemistry. *Acc. Chem. Res* **52**, 521-522 (2019).

[4] Perez, A. J. & Zeadally, S. Recent advances in wearable sensing technologies. *Sensors* **21**, 6828 (2021).

[5] Luo, Y. *et al.* Technology roadmap for flexible sensors. *ACS Nano* **17**, 5211-5295 (2023).

[6] Ates, H. C. *et al.* End-to-end design of wearable sensors. *Nat. Rev. Mater* **7**, 887-907 (2022).

[7] Jiang, Z. *et al.* Ultraflexible integrated organic electronics for ultrasensitive photodetection. *Adv. Mater. Technol* **6**, 2000956 (2021).

[8] Wei, B. B. *et al.* Ultraflexible tattoo electrodes for epidermal and in vivo electrophysiological recording. *Cell Rep. Phys. Sci.* **4**, 23 (2023).

[9] Skin to e-skin. *Nat. Nanotechnol.* **12**, 1017-1017 (2017).

[10] Someya, T. *et al.* A large-area, flexible pressure sensor matrix with organic field-effect transistors for artificial skin applications. *Proc. Natl. Acad. Sci.* **101**, 9966-9970 (2004).

[11] Wang, W. *et al.* Neuromorphic sensorimotor loop embodied by monolithically integrated, low-voltage, soft e-skin. *Science* **380**, 735-742 (2023).

[12] Liu, R., Wang, Z. L., Fukuda, K. & Someya, T. Flexible self-charging power sources. *Nat. Rev. Mater.* **7**, 870-886 (2022).

[13] Lu Yin, J. W. Wearable energy systems: what are the limits and limitations? *Natl. Sci. Rev.* **10** (2023).

[14] Yu, H., Li, N. & Zhao, N. How far are we from achieving self-powered flexible health

monitoring systems: an energy perspective. *Adv. Energy Mater.* **11**, 2002646 (2021).
[15] Liu, R. *et al.* An efficient ultra-flexible photo-charging system integrating organic photovoltaics and supercapacitors. *Adv. Energy Mater.* **10**, 2000523 (2020).
[16] Liu, R. *et al.* Silicon nanowire/polymer hybrid solar cell-supercapacitor: a self-charging power unit with a total efficiency of 10.5%. *Nano Lett.* **17**, 4240-4247 7b01154 (2017).

2) For the claim "This process results in an overall efficiency of 6.61%, which stands among the highest efficiencies reported for variable kinds of FEHSS", we have updated with more recent and relevant references, in response to the reviewer's suggestion. Additionally, we have introduced a new table in the Supplementary information (**Table S4**, as detailed below) that compares the performance of integrated photo-charging devices. Despite the limited number of work demonstrating decent performance, we have ensured to include all relevant studies in this comparison.

Table S4. Summary of the performance of reported FEHSSs based on solar energy harvesters and battery storage systems.

FEHSS type	1/Thickness (mm^{-1})	PCE (%)	Energy density ($mWh\ cm^{-2}$)	Specific capacity ($mAh\ cm^{-2}$)	Diode	Overall efficiency (%)	Ref.
PSC-ZIB	6.66	11.1	0.0016	-	No	5.28	26
PSC-ZIB	2.85	18.27	5.11	3.63	No	-	27
SiPV-LIB	0.77	15.8	2.7	0.5	No	7.61	28
SiPV-LIB	0.4	6	6.98	1.84	No	-	29
FIED	3.85	3.5	-	-	Yes	-	30
OPV-LIB	4.0	5.49	1.25	3.5	No	-	31
OPV-ZIB	11.1	16.18	5.82	3.88	Yes	6.91	This work

Note: PSC stands for perovskite solar cell, ZIB stands for zinc-ion battery, SiPV stands for silicon photovoltaic, LIB stands for lithium-ion battery, FIED stands for fiber-shaped integrated energy device, OPV stands for organic photovoltaic.

7. On page 14, line 372, what is polyvinyl alcohol (PVA-GO) hydrogel? Is it fully termed?

Author response:

We appreciate the reviewer for pointing this out. We have revised the text to include a proper definition of the abbreviation:

[page 15, line 15]

First, we introduced an ultrathin hydrogel electrolyte, i.e., 10 µm-thick poly(vinyl alcohol)/graphene oxide (PVA-GO) hydrogel, formed by a cold-lamination method we have previously reported.

We acknowledge the valuable suggestions from two reviewers, which have inspired us and aided in reorganizing the manuscript, thereby elevating its coherence and quality. We are confident that our revised manuscript offers enhanced relevance and applicability to a broader readership.

REVIEWERS' COMMENTS

Reviewer #1 (Remarks to the Author):

The revised manuscript is well re-organized based on the comments. I think it is suitable to be published in 'nature communications'.

By the way, please change the figure 4, which is unclear.

Reviewer #2 (Remarks to the Author):

The manuscript has been well improved. This reviewer recommends its publication in Nature Communications.

We thank the reviewers for recognizing the merits of our manuscript and providing valuable comments for further improvement. We have revised our article following the suggestions.

Response to Reviewers:

Reviewer #1 (Remarks to the Author):

The revised manuscript is well re-organized based on the comments. I think it is suitable to be published in 'nature communications'.
By the way, please change the figure 4, which is unclear.

<u>Author response:</u>

We appreciate the referee's positive assessment of our work and have addressed the comment point by point as detailed below.

As per the guidelines of the manuscript, we have removed the dashed box lines from Figure 4A, and have slightly modified Figure 4B as follows to enhance its clarity:

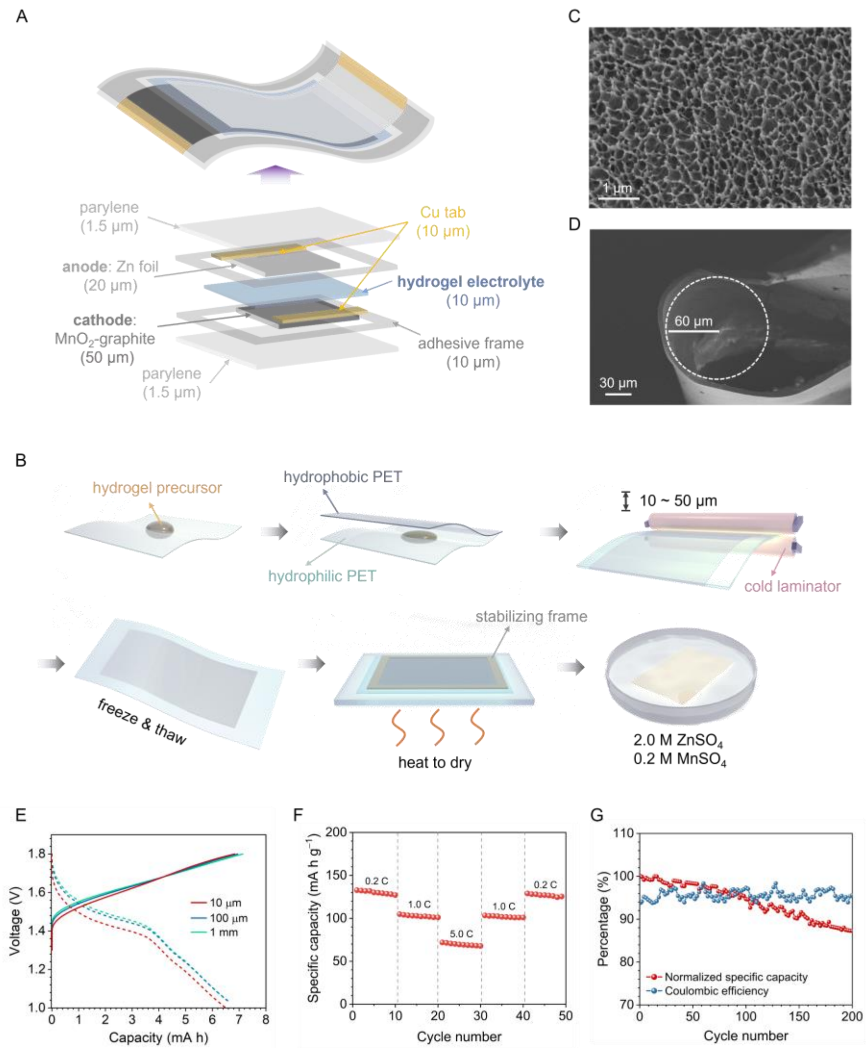

Reviewer #2 (Remarks to the Author):

The manuscript has been well improved. This reviewer recommends its publication in Nature Communications.

Author response:

We appreciate the referee's positive assessment of our work.

We acknowledge the valuable suggestions from two reviewers, which have inspired us and aided in reorganizing the manuscript, thereby elevating its coherence and quality. We are confident that our revised manuscript offers enhanced relevance and applicability to a broader readership.